Available online at www.sciencedirect.com
ScienceDirect
Journal of Nuclear Materials 363–365 (2007) 395–399
journal of nuclear materials
www.elsevier.com/locate/jnucmat

Contribution of hydrogen molecular assisted recombination processes to population of hydrogen atom in divertor simulator MAP-II

A. Okamoto [a,*], S. Kado [b], K. Sawada [c], Y. Kuwahara [d], Y. Iida [d], S. Tanaka [d]

[a] School of Engineering, Tohoku University, 6-6-01-2 Aobayama, Sendai 980-8579, Japan
[b] High Temperature Plasma Center, The University of Tokyo, 5-1-5 Kashiwanoha, Kashiwa 277-8568, Japan
[c] Faculty of Engineering, Shinshu University, 4-17-1 Wakasato, Nagano 380-8553, Japan
[d] School of Engineering, The University of Tokyo, 7-3-1 Hongo, Tokyo 113-8656, Japan

Abstract

Electron temperature and density of a hydrogen plasma are measured using laser Thomson scattering in divertor simulator MAP-II. Population of hydrogen atom calculated using the temperature and density are compared to that obtained from Balmer series emission spectroscopy, showing molecular assisted recombinations (MAR) contribute to populating process. One of the MAR, mutual neutralization following negative ion production is indicated by increase of $p = 3$ excited state, while dissociative recombination of molecular ion (H_2^+) increases $p = 4$–6 states.

PACS: 52.20.−j; 52.70.−m; 52.70.Kz; 39.30.+w

Keywords: Divertor plasma; Thomson scattering; Spectroscopy; Collisional-radiative model; MAP-II

1. Introduction

Understanding of molecular assisted recombination (MAR) processes in divertor plasmas is an important issue to achieve plasma detachment [1,2]. In hydrogen plasma, dissociative attachment (DA) of vibrationally excited molecular hydrogen followed by mutual neutralization (MN) assists recombination (referred to as 'DA-MAR') as well as ion conversion (IC) or charge-exchange (CX) followed by dissociative recombination (IC-MAR) [3]. These processes are summarized in Table 1. CX process in hydrogen plasma is not distinguished from IC process. On the other hand, suppression mechanisms of the MAR processes also exist, in which intermediately produced ions (H^- produced by DA, H_2^+ by IC) are destroyed by high-energy electron impact, for example. Thus measurements of the product in the final stage of the MAR are important as well as those of the intermediate products [4].

Population density of excited hydrogen atom can be indicative of mutual neutralization, because

* Corresponding author. Fax: +81 22 795 7900.
E-mail address: atsushi.okamoto@qse.tohoku.ac.jp (A. Okamoto).

0022-3115/$ - see front matter © 2007 Elsevier B.V. All rights reserved.
doi:10.1016/j.jnucmat.2007.01.033

Table 1
Molecular assisted recombination processes in hydrogen plasma. In reaction equation, $H_2(v)$ represent vibrationally excited molecule, H^*, an excited atom

	Label	Reaction
DA-MAR	DA	$H_2(v) + e \rightarrow H^- + H$
	MN	$H^- + H^+ \rightarrow H + H^*$
IC-MAR	IC, CX	$H_2(v) + H^+ \rightarrow H_2^+ + H$
	DR	$H_2^+ + e \rightarrow H + H^*$

hydrogen atom is selectively excited to $p = 2, 3$ states through this process, where p represents principal quantum number. However these excited states are affected by photon absorption from ground state atom. The effect of IC-MAR should also be considered, since the process generally has larger reaction rate than DA-MAR. For example, rate coefficient of IC-MAR is 6×10^{-11} cm^3/s (vibrational quantum number, $v = 0$) to 1×10^{-9} cm^3/s ($v = 4$), while DA-MAR, 1×10^{-12} cm^3/s ($v = 0$) to 4×10^{-11} cm^3/s ($v = 4$) for electron temperature $T_e = 2.0$ eV and electron density $n_e = 10^{15}$ cm^{-3} [5].

The population is determined by complicated balance of various atomic processes. In order to extract the contributions of the MAR processes to the population experimentally, reaction rates for the processes have to be evaluated. Thus electron temperature and density should be measured as well as hydrogen atom and molecule densities. Investigation of the recombining plasma requires reliable measurement methods for electron temperature applicable to low-temperature recombining plasmas, since reaction rate in low temperature plasma strongly depends on the electron temperature. While Langmuir probe method in recombining detached plasmas has sometimes anomaly in the current (I)–voltage (V) characteristics [6–9], laser Thomson scattering method is supposed to be an alternative candidate for this purpose. We developed a laser Thomson scattering system, which is equipped with a double monochromator to obtain narrow Doppler broadening, for the measurement of electron temperature in low-temperature recombining plasmas [10].

In the present paper, hydrogen-MAR in divertor simulator MAP (material and plasma)-II is investigated in terms of the final-stage product, i.e., excited hydrogen atom. In Section 2, experimental setup is described. Results and discussion are presented in Section 3. Then the paper is summarized in Section 4.

2. Experimental setup

The experiments were performed in the steady-state linear divertor/edge plasma simulator, MAP (Material and Plasma)-II [11–13]. The MAP-II device consists of two chambers jointed each other by a drift tube. The plasma, which is generated by DC arc discharge, is transmitted along an axial magnetic field of about 20 mT through a first chamber (source chamber) into a second chamber (gas target chamber). In the present experiment, hydrogen plasma in the first chamber is investigated, where relatively high-density plasmas are maintained.

A laser Thomson scattering system installed in the MAP-II device is described in Ref. [10]. Here we describe the system briefly. A frequency-doubled Nd:YAG laser (10 Hz, 500 mJ, 532 nm) beam is directed to a plasma with a mirror located beneath the chamber. A lens with a focal length of 1 m focuses the beam on the center of the plasma. Scattered light from a scattering volume is collected at 90° to both the magnetic field and the incident laser beam. An F/4.1 collection lens images the scattering volume onto a bundle fiber array, which transfers the light to a double-monochromator. An image-intensified charge-coupled device (ICCD) detects dispersed spectra. Wavelength resolution of the light detection system is 0.13 nm, while spatial resolution is 4.5 mm in radial direction in the present experiment. Scattering signal of 18 000 laser pulses (30 min) are accumulated for each plasma condition.

Passive spectroscopy of hydrogen atom and molecule emission also use the same collecting optics, while the plasma emission collected to a fiber transferred to a 1 m Czerny–Turner monochromator with a 2400 lines/mm grating and detected by a photomultiplier tube. Typical wavelength resolution in the present experiment is 0.02 nm. Intensity of Balmer series emission from 656 nm ($p = 3$ excited state) to 383 nm ($p = 9$) and Fulcher-α bands (600–640 nm) are observed.

Spatial distribution is obtained by changing t he height of the collecting optics, movable range of which is from the center to $r \simeq 15$ mm, covering core of the plasma column. To obtain local emission intensity from line-integrated emission, Abel inversion method is applied, where integral is performed up to $r = 40$ mm corresponding to radius about twice larger than the plasma column.

3. Results and discussion

Radial distribution of the electron temperature and that of the electron density measured using the laser Thomson scattering are shown in Fig. 1. The electron temperature $T_e(0) = 6.8$ eV and the density $n_e(0) = 2.3 \times 10^{12}$ cm^{-3} in the center are achieved in a typical discharge condition: a discharge voltage 90 V, a discharge current 30 A, and hydrogen gas injected to the arc discharge region with a flow rate 0.34 Pa m^3/s. Parabolic curves represent profile fitting: $T_e(r) \simeq 6.8 - 0.015r^2$ and $n_e(r) \simeq 2.3 \times 10^{12} - 0.67 \times 10^{10} r^2$, showing zero-cross points, $T_e \simeq 0$ at $r \simeq 21$ mm and $n_e \simeq 0$ at $r \simeq 19$ mm. Although the estimation is naive, these radii roughly correspond to sum of the cathode radius (15 mm) and Larmor radius of proton (7 mm for $T_i = 1$ eV, for example). Thus we extrapolate T_e and n_e with the parabolic curves to obtain those of $r = 15$ mm for input value in calculations.

Since the MAR rates are sensitive to vibrationally excited state of hydrogen molecule [14], rotational and vibrational temperatures of hydrogen molecule are evaluated. In order to obtain these temperatures, Fulcher-α band emission spectra are used with measured $T_e(r)$ and $n_e(r)$ [15]. The rotational and vibrational temperature are determined to be $T_{rot} = 700$ K and $T_{vib} = 6000$ K, respectively, where the radial distribution of these temperatures are almost constant in the plasma column.

To estimate contribution of MAR to population of excitation state of hydrogen atom, atom/molecule density ratio (or dissociation degree, equivalently) should be determined. In the present experiment, it is determined from Balmer/Fulcher emission ratio [4], and the resulting atom/molecule density ratio is about $F = 0.35 \pm 0.1$ inside $r = 15$ mm. Then the densities of atomic and molecular hydrogen, n_H and n_{H_2}, respectively, are determined by following equations:

$$F = n_H / n_{H_2}, \tag{1}$$

$$p = n_H T_H + n_{H_2} T_{H_2}. \tag{2}$$

Total pressure, p, is considered as that measured at the chamber wall, $p = 1.2$ Pa. Atomic temperature, T_H, is assumed to be 0.6 eV, while molecular temperature, T_{H_2}, is the same as the rotational temperature, 700 K. Here we chose the atomic temperature so as to be enough higher than the molecular temperature and to be enough lower than dissociation energy of molecular hydrogen. Thus the atomic density $n_H = 9.8 \times 10^{12}$ cm^{-3} and molecular density $n_{H_2} = 2.8 \times 10^{13}$ cm^{-3} are obtained.

With these experimentally obtained temperatures (T_e, T_{vib}, T_{rot}) and densities (n_e, n_H, n_{H_2}), densities of ions (H^-, H^+, H_2^+, H_3^+) are determined by source balance equation with charge neutrality condition. Radial distributions of the ions shown in Fig. 2 indicate a major ion is proton. Substantial amount of molecular ion H_2^+ produced by IC exists as the intermediate ion of the MAR process, while negative ion H^- produced by DA is minority. We also note that the density of H_3^+ is the same order as that of H_2^+ and much smaller than proton in the present experiments. Thus the contribution from H_3^+ related

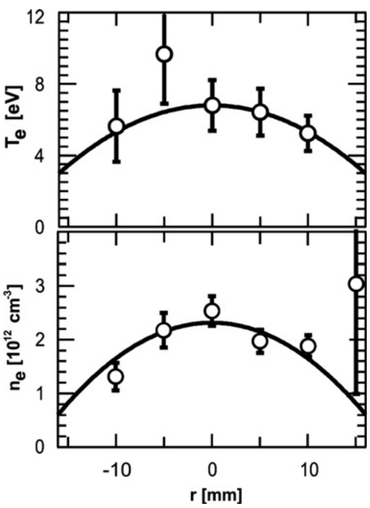

Fig. 1. Radial distributions of electron temperature and density measured by laser Thomson scattering.

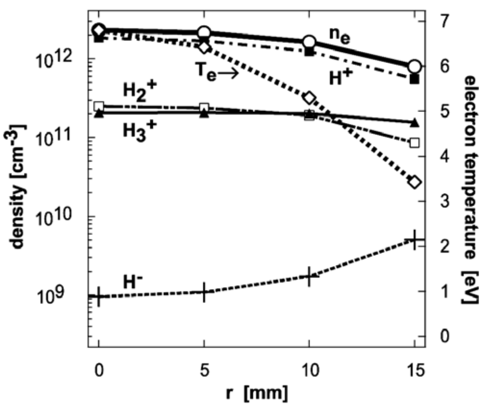

Fig. 2. Radial distribution of ion and electron densities calculated from source balance equation. Electron temperature is also shown for reference.

processes to the population of hydrogen atom is negligibly small.

Then collisional radiative (CR) model is applied to determine the population density of hydrogen atom. The CR model is based on Ref. [16], and includes MAR processes [5]. Ion temperature $T_i \simeq 0.1\ T_e$ is assumed for H^+ related processes (IC, MN). Radiative transport is also calculated [17], where absorption of Lyman series emission up to $p = 10$ is considered. Population balance due to emission and absorption is solved iteratively.

Population densities can be independently determined only using the Balmer emission intensities in the same experiment, where radial distribution is obtained using Abel inversion method. Comparison between the population densities of hydrogen atom obtained from the CR model and that from the emission intensities are shown in Fig. 3, where the experimental ones are normalized to the calculation at $p = 4$ state. The calculation well agrees with the experimental result. Although excitation from ground state atom (ex) dominates populating process, the total population density is clearly higher than that from ex process. The population increasing from that of ex process in $p > 4$ state is mainly caused by the IC-MAR processes. Contribution of the IC-MAR process accounts for 14% of total population in $p = 6$ state, while it decreases in $p = 3$ and $p \geqslant 7$ states. Comparing population density in the center of the plasma (Fig. 3(a), $T_e = 6.8$ eV and $n_e = 2.3 \times 10^{12}\ \mathrm{cm}^{-3}$) to that in peripheral region (Fig. 3(b), $T_e = 3.4$ eV and $n_e = 0.8 \times 10^{12}\ \mathrm{cm}^{-3}$), dependence of the IC-MAR process on T_e and n_e is rather weak.

In $p = 3$ state, while contribution of dissociative excitation ($H_2 + e \rightarrow H + H^* + e$) follows that of the excitation from atomic ground state in the center of the plasma (Fig. 3(a)), photon absorption and DA-MAR are secondary important processes in peripheral region (see Fig. 3(b)). The population caused by MN, which is known as $p = 2,3$-selective populating process, reaches about 18% of total population in the peripheral region. The calculated total population in $p = 3$ state is 24% higher than that of the experiment in the center of the plasma, and 35% higher in the peripheral region. About the overestimation of $p = 3$ population, we consider the following: (i) The effect of movement of ions is ignored in the CR model calculation, while the actual ions move away. Considering the transport of negative ion [4,18] reduce MN rate resulting in decreasing of $p = 3$ population. (ii) The negative ion could vanish in mutual neutralization with H_3^+. Since few reliable cross section of the process has been reported, the process cannot be included in the calculation. Considering the process as well as the transport of negative ion will also improve $p = 3$ population. (iii) The contribution of radiation transfer ($H(1) + h\nu_{13} \rightarrow H(3)$), which is also important process in the population in low electron-temperature and low electron-density region, is affected by atomic temperature. The atomic temperature is assumed to be constant ($T_H \simeq 0.6$ eV) from the core plasma to chamber wall. To check the assumption we calculate the atomic temperature using a Monte Carlo simulation code developed by Sawada and Goto.

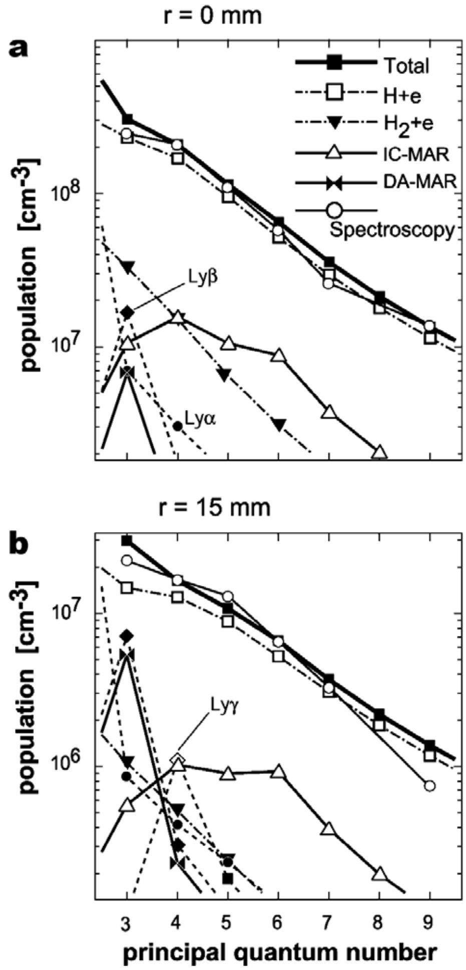

Fig. 3. Population density dependence on principal quantum number in $r = 0$ mm (a) and $r = 15$ mm (b). Filled square represents total population from CR model calculation; open square, electron collision excitation; filled triangle, dissociative excitation; open triangle, IC-MAR; pair triangle, DA-MAR; filled circle, Lyman-α absorption; filled diamond, Ly_β; open diamond, Ly_γ; and open circle, Balmer emission spectroscopy.

The code, which includes atom–molecule and molecule–molecule elastic collision, was originally written for transport calculation on hydrogen atom and molecule in the Large Helical Device. Then $T_H \simeq 0.2$ eV out of the plasma column are obtained. The assumption is partly overestimated resulting in underestimation of $p = 3$ population. Therefore this is not the reason. Quantitative understanding of $p = 3$ overestimated population remains to be our future work.

4. Summary

Electron temperature and density of a hydrogen plasma are measured using laser Thomson scattering in divertor simulator MAP-II. Rotational and vibrational temperature of hydrogen molecule are obtained from Fulcher-α emission spectroscopy with the electron temperature and density. Populations of hydrogen atom are obtained from a collisional radiative model including molecular assisted recombination (MAR) processes and radiative transfer. The populations are compared to that obtained from Balmer emission spectroscopy, showing MARs contribute to populating processes. One of the MAR, mutual neutralization following negative ion production is indicated by increase of $p = 3$ excited state, accounting for 18% of total population in a low temperature ($T_e = 3.4$ eV) and low density ($n_e = 0.8 \times 10^{12}$ cm^{-3}) plasma. On the other hand, dissociative recombination of molecular ion (H_2^+) increases $p = 4$–6 states, which reaches up to 14% of total population even in a relatively high temperature ($T_e = 6.8$ eV) and high density ($n_e = 2.3 \times 10^{12}$ cm^{-3}) plasma. Overestimation of $p = 3$ state population implies reduction of MAR rate caused by transport and destruction of hydrogen negative ion.

Acknowledgements

This work was partly supported by the Ministry of Education, Culture, Sports, Science and Technology of Japan (MEXT) Grant-in-Aid for Young Scientists (B), 17740362, 2005 for the first author, 16740311, 2004 for the second author. This work was also supported in part by a NIFS Collaborative Research Program (NIFS04KOAB009) directed by the second author.

References

[1] N. Ohno, N. Ezumi, S. Takamura, S.I. Krasheninnikov, A.Y. Pigarov, Phys. Rev. Lett. 81 (1998) 818.
[2] J.L. Terry, B. Lipschultz, A.Y. Pigarov, S.I. Krasheninnikov, B. LaBombard, D. Lumma, H. Ohkawa, D. Pappas, M. Umansky, Phys. Plasmas 5 (1998) 1759.
[3] S.I. Krasheninnikov, A.Y. Pigarov, D.J. Sigmar, Phys. Lett. A 214 (1996) 285.
[4] S. Kado, S. Kajita, D. Yamasaki, Y. Iida, B. Xiao, T. Shikama, T. Oishi, A. Okamoto, S. Tanaka, J. Nucl. Mater. 337&339 (2005) 166.
[5] K. Sawada, T. Fujimoto, Contribution Plasma Phys. 42 (2002) 603.
[6] R.D. Monk, A. Loarte, A. Chankin, S. Clement, S.J. Davies, J.K. Ehrenberg, H.Y. Guo, J. Lingertat, G.F. Matthews, M.F. Stamp, P.C. Stangeby, J. Nucl. Mater. 241&243 (1997) 396.
[7] N. Ezumi, N. Ohno, K. Aoki, D. Nishijima, S. Takamura, Contribution Plasma Phys. 38 (1998) S31.
[8] N. Ohno, N. Tanaka, N. Ezumi, D. Nishijima, S. Takamura, Contribution Plasma Phys. 41 (2001) 473.
[9] A. Okamoto, S. Kado, Y. Iida, S. Tanaka, Contribution Plasma Phys. 46 (2006) 416.
[10] A. Okamoto, S. Kado, S. Kajita, S. Tanaka, Rev. Sci. Instrum. 76 (2005) 116106.
[11] H. Kobayashi, S. Kado, B. Xiao, S. Tanaka, Jpn. J. Appl. Phys. 42 (2003) 1776.
[12] S. Kado, H. Kobayashi, T. Oishi, S. Tanaka, J. Nucl. Mater. 313&316 (2003) 754.
[13] S. Kado, Y. Iida, S. Kajita, D. Yamasaki, A. Okamoto, B. Xiao, T. Shikama, T. Oishi, S. Tanaka, J. Plasma Fus. Res. 81 (2005) 810.
[14] J. Wadehra, J. Birdsley, Phys. Rev. Lett. 41 (1978) 1795.
[15] B. Xiao, S. Kado, S. Kajita, D. Yamasaki, Plasma Phys. Control. Fus. 46 (2004) 653.
[16] T. Fujimoto, K. Sawada, K. Takahata, J. Appl. Phys. 66 (1989) 2315.
[17] K. Sawada, J. Plasma Phys. 72 (2006) 1025.
[18] S. Kado, S. Kajita, T. Shikama, Y. Iida, D. Yamasaki, A. Okamoto, S. Tanaka, Contribution Plasma Phys. 46 (2006) 367.